

Articles

Structure-Based Design and Synthesis of 2-Benzylidene-benzofuran-3-ones as Flavopiridol Mimics

Joseph Schoepfer,* Heinz Fretz, Bhabatosh Chaudhuri, Lionel Muller, Egge Seeber, Laurent Meijer,[§] Olivier Lozach,[§] Eric Vangrevelinghe, and Pascal Furet*

Oncology Research, NOVARTIS Pharma AG, 4002 Basle, Switzerland

Received February 1, 2001

Novel 2-benzylidene-benzofuran-3-ones were designed and synthesized to mimic flavopiridol, a well-established inhibitor of cyclin-dependent kinases (CDKs) which is currently undergoing clinical evaluation. The underlying design concepts as well as the synthesis and structure–activity relationships (CDKs 1, 2, and 4 enzyme assays) of these mimics are described. Inhibitors of CDKs 1 and 2 that are more potent and selective than flavopiridol were obtained.

Introduction

The inhibition of cyclin-dependent kinases (CDKs) has emerged as an important theme in anticancer agents research.^{1–5} Compounds able to inhibit the activity of these crucial enzymes in the regulation of the cell division cycle are expected to have antiproliferative properties. Among the various small molecule CDK inhibitors that have been reported, flavopiridol (**1**) is the most advanced in therapeutic investigations.^{6,7} The compound has completed phase I clinical trial where it has showed antitumor effect in patients with refractory neoplasms.⁸ This encouraging result, which is consistent with the ability of **1** to inhibit the proliferation of cancer cells in vitro, has triggered further medicinal chemistry work in the series.^{9,10} One possible area of improvement is selectivity since, unlike most of the reported CDK inhibitors, **1** inhibits the most firmly established oncology targets CDKs 1, 2, and 4 with the same level of potency.¹¹ These enzymes are involved at different stages of the cell cycle. More selective inhibitors would therefore provide a broader palette of biological profiles.

In this paper, we report efforts in this direction using a designed 2-benzylidene-benzofuran-3-one scaffold to mimic the flavonoid structure of **1**.

Design

The structural basis of the CDK inhibitory activity of **1** has been elucidated by an X-ray crystal structure of CDK2 in complex with its *des*-chloro analogue.¹² Very recently, the crystal structure of CDK2 ligated by **1** itself was also reported.¹⁰ These structures show that the chromenone moiety of the inhibitor acts as a mimetic of the purine moiety of ATP, the cofactor of the enzyme (Figure 1). In particular, the 4-keto and 5-hydroxy

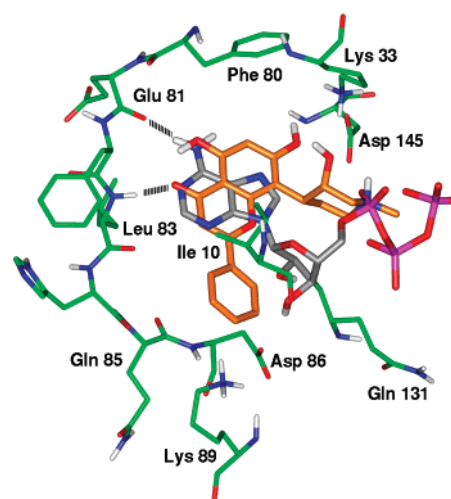


Figure 1. Relative binding modes of ATP (gray) and the *des*-chloro analogue of flavopiridol (orange) in the CDK2 active site. The hydrogen bonds formed with Glu 81 and Leu 83 are indicated as dashed lines.

groups of the compound establish the same bidentate hydrogen bonds with the backbone of CDK2 residues Leu 83 and Glu 81¹³ as the nitrogen atoms at positions 1 and 6 of the purine moiety of ATP. Moreover, the piperidinyl moiety interacts with conserved residues of the catalytic cleft that are normally used to bind the ribose ring and the phosphate chain of ATP. In contrast, the phenyl ring in position 2 of the chromenone moiety forms interactions with CDK2 that are not observed in the complex with ATP.¹⁴ These additional interactions mainly consist in hydrophobic contacts with the side chain of Ile 10.

On the basis of this information, we reasoned that a 4-hydroxy benzofuranone structure (Chart 1) should be able to mimic the 5-hydroxy chromenone moiety of **1** in its binding interactions with CDKs. Position 7 of the benzofuranone would then naturally match position 8 of the chromenone for piperidinyl group attachment. To introduce a pendant to the phenyl substituent of **1**,

* Corresponding authors: J. Schoepfer (tel, 41 61 696 36 09; fax, 41 61 696 62 46; e-mail, joseph.schoepfer@pharma.novartis.com) or P. Furet (tel, 41 61 696 79 90; fax, 41 61 696 27 61; e-mail, pascal.furet@pharma.novartis.com).

[§] CNRS, Cell Cycle Group, Station Biologique, BP 74, Roscoff 29682 Cedex, France.

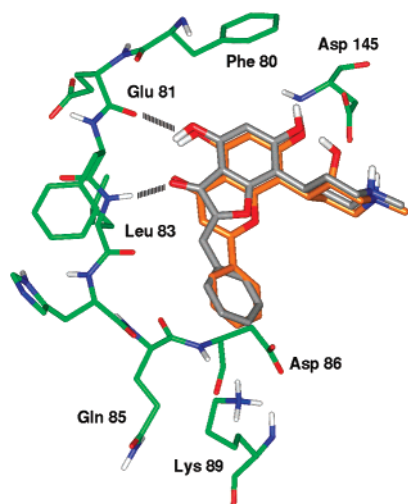
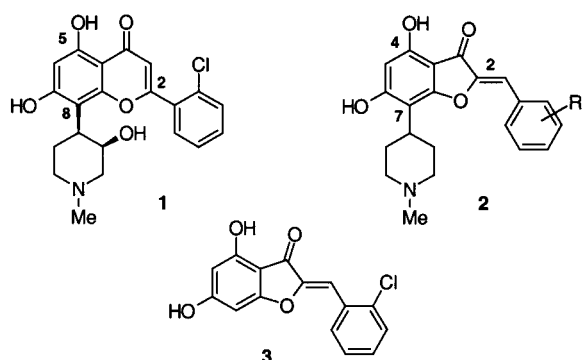


Figure 2. Overlay of the *des*-chloro analogue of flavopiridol (orange) and the benzofuranone mimic (gray) docked in the ATP binding site of CDK2. The hydrogen bonds formed with Glu 81 and Leu 83 are indicated as dashed lines.

Chart 1. Flavopiridol (**1**), Designed Benzofuranone Mimics **2**, and Related Compound **3** Retrieved from the Novartis Compound Collection

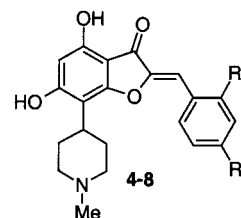


whose exact corresponding position of attachment is missing in the benzofuranone, a modeling experiment suggested that an exocyclic double bond in position 2 be used as a spacer. This is illustrated in Figure 2 with an overlay of the designed benzofuranone scaffold **2** and the *des*-chloro analogue of **1** in the ATP binding site of CDK2. The hydroxyl group of the piperidinyl ring was omitted in the mimic for easier synthetic access. In fact, it has been shown that this hydroxyl group is not very critical for CDK inhibitory activity.⁹

Before committing chemistry, we sought to validate the mimetic concept by testing existing compounds retrieved from the Novartis chemical archives. Thus, a 2-D substructure search of the compound collection using 2-benzylidene-benzofuran-3-one as query was conducted. The search returned several benzofuranone derivatives that were tested in our CDK2 and CDK4 inhibition assays. One of them, compound **3**, showed significant activity at the entry concentration of 50 μ M (80% and 40% inhibition of CDK4 and CDK2, respectively). Considering that **3** lacked the piperidinyl moiety of **1**, which is seen to make favorable interactions with CDK2 in the crystal structures, this result encouraged us to undertake the synthesis of the envisaged target structures **2**.

Our main objective was to obtain new CDK inhibitors that are more selective than **1**. In particular, discrimi-

Table 1. Binding Energies (kcal/mol) for Benzofuranone Mimics and Flavopiridol



no.	R ¹	R ²	E_{binding}^a
4	H	H	-17.8
5	H	Cl	-16.0
6	NO ₂	H	-19.0
7	SO ₂ NH ₂	H	-20.6
8	Me-Pip ^b	H	-14.4
1	flavopiridol (1)		-19.3

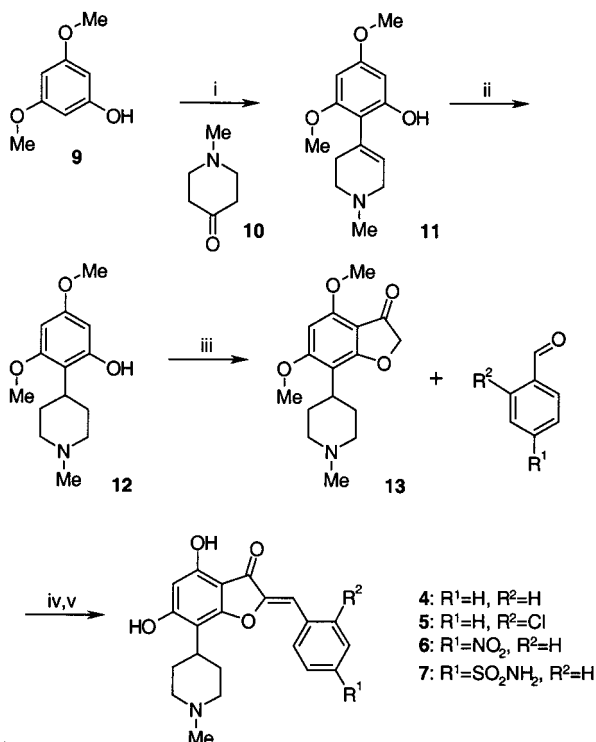
^a Binding energy calculated by means of eq 1. ^b 4-Methyl-piperazin-1-yl.

nation between CDK2 and CDK4 was desired. To this end, we used the model shown in Figure 2 to select specific R substituents for the phenyl ring attached by a double bond to position 2 of the benzofuranone bicycle. As can be seen in the figure, this phenyl ring is proximal to Lys 89, one of the few residues of the ATP binding site of CDK2 that are not conserved in CDK4 (Lys 89 corresponds to Thr 102 of CDK4). Modeling suggested that a hydrogen bond acceptor group in para position of the phenyl ring would interact favorably with the side chain amino group of Lys 89 in CDK2 but not with the shorter and less polar side chain of Thr 102 in CDK4, thus favoring binding to CDK2. Conversely, introduction of a bulky and positively charged para substituent was expected to have a detrimental effect on the affinity for CDK2, but not on that for CDK4, by creating a repulsive interaction with Lys 89. The R substituents were selected on the basis of this concept. In particular, a *p*-sulfonamide substituent was envisaged to reinforce binding to CDK2. In addition, to accept hydrogen bonds from Lys 89 (oxygen atoms of the sulfonamide), as previously explained, this group could also donate a hydrogen bond to the proximal Asp 86 residue (amino group of the sulfonamide) in a modeling experiment.¹⁵

Calculation of the CDK2 binding energies of the envisaged compounds gave support to these qualitative modeling ideas. The results of the calculations, based on molecular mechanics and a water solvation model as described in the Experimental Section, are reported in Table 1. In agreement with the design concept, the most favorable binding energy (-20.6 kcal/mol) was obtained with the sulfonamide substituent whereas the introduction of a positively charged 4-methyl-piperazin-1-yl group was calculated to be destabilizing, the binding energy increasing by 3.4 kcal/mol compared to the unsubstituted reference compound **4**.

Chemistry

2-Benzylidene-4,6-dihydroxy-7-(1-methyl-piperidin-4-yl)-benzofuran-3-ones **4–8** were synthesized from 4,6-dimethoxy-7-(1-methyl-piperidin-4-yl)-benzofuran-3-one **13** and a substituted benzaldehyde via base-catalyzed aldol condensation (Scheme 1).¹⁶ The reaction is known to proceed stereoselectively and afford the (*Z*)-aurone derivative.^{17,18} The dimethoxy intermediates

Scheme 1. Synthesis of Benzofuranone Derivatives 4–7^a

^a Reagents and conditions: (i) HCl gas, acetic acid, 25 °C, 24 h; (ii) H₂, Pd/C, acetic acid–water, 25 °C, 20 h; (iii) chloroacetyl chloride, AlCl₃, 0–100 °C, 1 h; (iv) KOH, ethanol, 25 °C, 1 h; (v) pyridinium hydrochloride, 180 °C, 3 h.

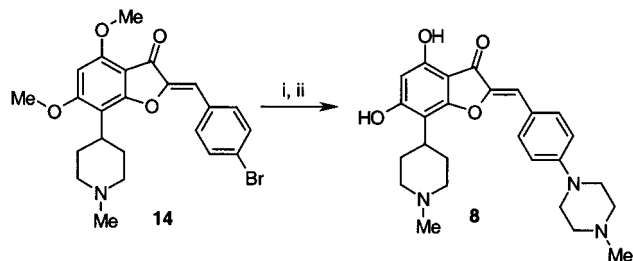
were treated with pyridinium hydrochloride accordingly to the patent procedure for flavopiridol derivatives,¹⁹ and the final products were purified using reverse phase MPLC.

The acid-catalyzed condensation of dimethoxy phenol **9** and 1-methyl-4-piperidone **10** in acetic acid afforded the unsaturated derivative **11** in 62% yield.¹⁹ The compound **11** was then hydrogenated to afford **12**, which was treated successively with chloroacetyl chloride and aluminum trichloride in a one-pot procedure to afford the benzofuranone **13** derivative in 50% yield. This compound **13** was then condensed with commercially available benzaldehyde derivatives and synthesized 4-formylbenzenesulfonamide²⁰ in ethanol in the presence of 2 equiv of potassium hydroxide. The dimethoxy derivatives were directly deprotected with pyridinium hydrochloride at 180 °C. Purification using a C₁₈ reverse phase column with a 0.1% aqueous TFA and 0.1% TFA in acetonitrile solvent systems afforded, after lyophilization, TFA salts of compounds **4–7** (Scheme 1).

The piperazine derivative **8** was obtained in three steps. First, **13** was condensed with 4-bromobenzaldehyde to afford **14** in 41% yield using the above-described procedure. The aryl bromide derivative **14** was then reacted with 1-methylpiperazine under Buchwald amination conditions (racemic-BINAP, Pd₂(dba)₃, Cs₂CO₃).²¹ The piperazine intermediate obtained in a 55% yield was deprotected using pyridinium hydrochloride to afford compound **8** in 40% yield (Scheme 2).

Results and Discussion

Compounds **4–8** were tested in kinase inhibition assays. These included CDKs 1,²² 2, and 4 (activated

Scheme 2. Synthesis of Benzofuranone Derivative **8**^a

^a Reagents and conditions: (i) 1-methylpiperazine, Pd₂(dba)₃, racemic-BINAP, cesium carbonate, dioxan, reflux, 12 h; (ii) pyridinium hydrochloride, 180 °C, 3 h.

Table 2. Enzyme Inhibition and Selectivity Profile of Benzofuranone Mimics and Flavopiridol

no.	IC ₅₀ [μM] ^a				% inhib at 10 μM		
	CDK1 /B	CDK2 /A	CDK4 /D1	GSK-3	PKCα	VEGF-KDR	EGFR
4	0.11	1.28	4.41	4.2	19	2	38
5	0.60	3.97	25.25	10.0	22	17	1.68 ^b
6	0.06	0.31	2.21	4.8	22 ^b	37	43
7	0.009	0.03	1.87	3.7	42	25	36
8	0.80	2.98	1.92	1.75	21	25	29
1	0.10	0.22	0.40	0.45 ^c	23 ^b	>10 ^b	4.6 ^b

^a The data represent averages of at least three determinations. ^b IC₅₀ [μM]. ^c From literature.²³

by cyclin B, A, and D1, respectively) and four kinases not belonging to the CDK family: GSK-3,²³ PKCα,²⁴ KDR,²⁵ and EGF-R.²⁶ The data are reported in Table 2 in comparison with the corresponding inhibition profile of flavopiridol (**1**).

The unsubstituted reference compound **4** turned out to inhibit CDK1 as potently as **1** but was weaker than the latter in inhibiting CDK2 and CDK4. In our model, **4** exclusively interacts with residues that are conserved in CDKs 1, 2, and 4. Thus, the higher potency of **4** against CDK1 is likely to reflect an intrinsic difference in the sensitivity of the CDK1 assay compared to the CDK2 and CDK4 ones. Nevertheless, the overall data for **4** provided the first confirmation that the benzofuranone mimetic concept worked since significant inhibition of the CDKs was achieved while keeping high selectivity against kinases outside the CDK family with the exception of GSK-3, a profile previously observed with CDK inhibitors.²³

Introduction of an ortho chloro substituent (compound **5** compared to **4**) did not lead to the beneficial effect observed in the flavopiridol series.²⁷ On the contrary, some potency against the three CDK enzymes was lost. The recently published crystal structure of CDK2 in complex with **1** offers a basis to explain this effect.¹⁰ In the CDK2-bound conformation of **1**, the ortho chloro substituent has a syn orientation with respect to the O1 atom of the benzopyran ring. In this orientation, the chlorine atom makes a favorable hydrophobic contact with the side chain of Ile10. The geometry of the benzofuranone mimic does not allow an ortho substituent on the phenyl ring to be syn with respect to the pendant O1 atom of the benzofuranone moiety. In the syn conformation, there is steric hindrance between the substituent and the O1 atom, which leads to deconjugation of the molecule. As a consequence, **5** has to adopt the anti conformation which is less favorable for binding to CDKs as suggested by the crystal structure of CDK2

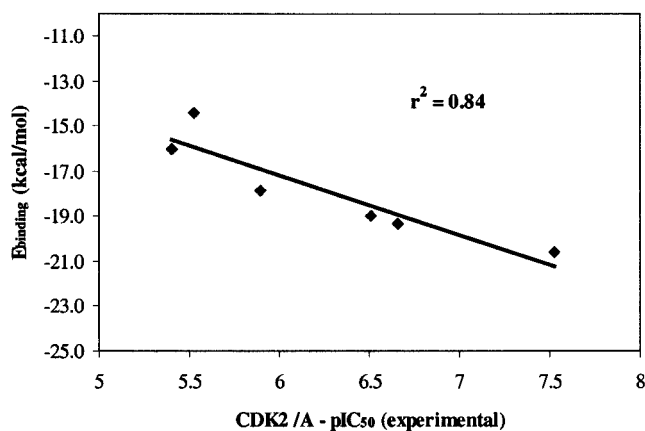


Figure 3. Correlation between inhibitory activities (pIC₅₀) in the CDK2/cyclin A assay (Table 2) and calculated binding energies (Table 1). The solid line represents the linear tendency.

in complex with **1** and also by our binding energy calculations.

As testified by the inhibition data of compounds **6** and **7**, targeting Lys 89 for hydrogen bond interactions with a para acceptor substituent was a successful strategy to increase CDK2 inhibitory activity. Compounds **6** and **7** are significantly more potent than **4** in inhibiting CDK2, whereas no marked effect is observed on the activity against CDK4 in which the lysine is not conserved. Moreover, **6** and **7** are also more potent than **4** in inhibiting CDK1 which is consistent with the conservation of the lysine residue in this enzyme. A comparison of the relative CDK2 activities of **6** and **7** suggests that the targeted additional hydrogen bond interaction with Asp 86 was realized. The increase in potency obtained by changing the substituent from nitro to sulfonamide can be ascribed to the additional capacity of the sulfonamide group to donate hydrogen bonds. The CDK1 inhibitory potencies of **6** and **7** follow the same trend. This was not unexpected since Asp 86 is conserved within the CDK family.

The 4-methyl-piperazin-1-yl substituent has a deleterious influence on the CDK1 and CDK2 potencies (compound **8** compared to **4**). The effect, more apparent in the case of CDK1, is in agreement with our concept of creating a repulsive interaction with Lys 89. However, we expected it to be stronger. The conformational flexibility of its side chain probably allows Lys 89 to avoid a very unfavorable steric and electrostatic interaction with the bulky basic substituent. No significant change in CDK4 potency was observed for **8** compared to **4**, which indicates that replacement of Lys 89 by a threonine in this enzyme allows the 4-methyl-piperazin-1-yl substituent to access freely the solvent space as suggested by modeling.

It was satisfying to observe that the computed CDK2 binding energies of the inhibitors exhibited overall a high correlation ($r^2 = 0.84$) with the experimental activity data (pIC₅₀) (Figure 3). In the present case, which deals with conformationally rigid and structurally very close analogues, a simple molecular mechanics approach appears to be adequate for predicting a correct ranking of the relative potencies.

Compounds **4–8** were also tested for antiproliferative activity in a HCT116 (transformed colon cell line) in

Table 3. Effect on Cell Proliferation of Derivatives **4–8**

no.	HCT-116 IC ₅₀ [μ M]
4	> 50
5	20.1
6	35.6
7	> 50
8	24.8

vitro cellular assay.²⁸ The data reported in Table 3 indicates that some antiproliferative activity was obtained with several of the compounds. This, in addition to the fact that structurally related (*E*)-2-benzylidene-1-indanone compounds have recently been reported to have potent cellular effects,³² is encouraging for further optimization efforts.

Conclusion

Compounds derived from the general structure 2-benzylidene-4,6-dihydroxy-7-(1-methyl-piperidin-4-yl)-benzofuran-3-ones designed as flavopiridol mimetics showed significant inhibition of CDKs 1, 2, and 4 enzymatic activities. Following a structure-based approach, it was possible to improve the CDKs 1 and 2 inhibitory activities of this class of compounds and obtain selectivity against CDK4. The reverse was not possible due the nature of the CDK4 ATP binding site that offers fewer opportunities than those of CDKs 1 and 2 to create strong favorable interactions with a ligand. Further characterization of these new CDK inhibitors is ongoing to determine their potential as antiproliferative agents.

Experimental Section

Enzyme Inhibition Assays.^{28–31} CDK4 and CDK2 kinase reactions were performed in buffer (25 mM MOPS pH 7.2, 1 mM MgCl₂·6H₂O, 15 mM EGTA, 1 mM DTT, 60 mM β -glycerophosphate, 30 mM *p*-nitrophenyl phosphate, 0.1 mM sodium orthovanadate) in a 50 μ L volume at 37 °C in V-form 96-well plates, at a final ATP concentration of 7.5 μ M. Benzofuranone derivatives **4–8** were used as 10 \times solutions in 10% DMSO (final concentration as 1%). GST-pRb(152) representing the C-terminal 152 amino acid fragment of pRb was used as a substrate for all enzymes along with 0.1 μ Ci of radioactive ³³P dATP. The reaction time was 60 min for CDK4 and 30 min for CDK2. The reactions were terminated by adding 20 μ L of 0.5 M EDTA pH 7.5. All assays were performed in duplicate and represent an average of three independent experiments. The CDK1/cyclin B assay is described in ref 31.

Chemistry. All starting materials were obtained from commercial sources unless otherwise specified in the Experimental Section. Preparative MPLC was done using a C₁₈ column (Merck LICHROPREP RP-18, 15–25 μ m; detection at 215 nm) and binary solvent systems, where A = 0.1% aqueous TFA and B = 0.1% TFA in acetonitrile. HPLCs were conducted using a SpectraSystem P4000 pump, a Nucleosil 100-5 C₁₈ (250 \times 4 mm) column, UV detection with a SpectraSystem UV2000 spectrometer at 214 nm, and a linear solvent gradient from 2% B to 100% B over 10 min, then 3 min 100% B, flow rate 2.0 mL/min. Proton magnetic resonance (NMR) spectra were recorded on Bruker 400 and 500 spectrometers and are reported in ppm relative to TMS and referenced to the solvent in which they were run. LC-MSs were done using binary solvent systems C = 0.05% aqueous TFA and D = 0.045% TFA in acetonitrile, with a Carlo Erba Phoenix 40 pump, a Phenomenex Luna 3 μ m C₁₈ (100 \times 1 mm) column, a linear solvent gradient from 5% B to 99% C over 9 min, then 1 min 100% D, flow rate 75 μ L/min; UV detection with MD 915 Jasco spectrometer at 214 nm, MS detection with a Micromass Quattro II spectrometer. Mass spectra were obtained on a

Micromass Platform II spectrometer, and high-resolution mass spectra were obtained on a Finnigan MAT 900 spectrometer.

3,5-Dimethoxy-2-(1-methyl-1,2,3,6-tetrahydro-pyridin-4-yl)-phenol (11).¹⁹ HCl gas was bubbled through a mixture of dimethoxy phenol (19.7 g, 128 mmol) and 1-methyl-4-piperidone (15.2 g, 140 mmol) in acetic acid (120 mL) for 1 h. The reaction mixture was stirred at room temperature for 24 h, the solvent was removed under reduced pressure, and recrystallization of the residue from ethanol/ether afforded the hydrochloride salt of **11** as a yellowish solid (17.9 g, 62%): mp 222–229 °C; HPLC t_R = 4.4 min; ¹H NMR (200 MHz, CDCl₃) δ 6.14 (d, 1 H), 6.02 (d, 1 H), 5.72 (m, 1 H), 3.76 (s, 3 H), 3.72 (s, 3 H), 3.12 (m, 2 H), 2.67 (m, 2 H), 2.42 (br s, 5 H); MS (ESI) m/z 250 [M + H⁺].

3,5-Dimethoxy-2-(1-methyl-piperidin-4-yl)-phenol (12). Compound **11** (17.9 g, 57.6 mmol) was hydrogenated in acetic acid–water (10:1, 220 mL) over Pd/C (1.8 g) at normal pressure and room temperature for 20 h. The reaction mixture was filtered over Celite, the solvent evaporated under reduced pressure, and recrystallization of the residue from ethanol afforded the hydrochloride salt of **12** as a white solid (15.8 g, 87%): mp 235–237 °C; HPLC t_R = 4.9 min; IR (KBr) 2918, 2800, 1603, 1507 cm⁻¹; ¹H NMR (400 MHz, CDCl₃) δ 11.25 (br s, 1 H), 6.02 (d, J = 2.3 Hz, 1 H), 5.91 (d, J = 2.3 Hz, 1 H), 3.78 (s, 3 H), 3.76 (s, 3 H), 3.15–2.90 (m, 5 H), 2.46 (s, 3 H), 2.14 (m, 2 H), 1.48 (m, 2 H); ¹³C NMR (100 MHz, CDCl₃) δ 159.0, 158.9, 158.4, 112.6, 94.9, 89.6, 57.3, 55.9, 55.1, 46.6, 31.7, 27.6; MS (ESI) m/z = 252 [M + H⁺].

4,6-Dimethoxy-7-(1-methyl-piperidin-4-yl)-benzofuran-3-one (13). Chloro-acetyl chloride (6.3 mL) was added dropwise to **12** (6.6 g, 21.2 mmol) at 0 °C. The mixture was stirred for 3.5 h at 50 °C and cooled to 0 °C, and aluminum trichloride (6.6 g, 49.4 mmol) was added in small portions. The reaction mixture was finally stirred for 1 h at 100 °C, cooled to room temperature, and quenched with an ice–water solution. The aqueous solution was neutralized with sodium hydrogencarbonate and extracted with DCM. The combined organic layers were dried over sodium sulfate, filtered, and concentrated under reduced pressure. Flash chromatography of the residue on silica gel eluting with DCM/methanol/ammoniac (9:1:0.1) gave the desired benzofuranone **13** as a white solid (3.1 g, 50%): mp 203–209 °C; HPLC t_R = 4.1 min; IR (DCM) 2941, 2846, 2786, 1699, 1617, 1596 cm⁻¹; ¹H NMR (400 MHz, CDCl₃) δ 6.04 (s, 1 H), 4.57 (s, 2 H), 3.96 (s, 3 H), 3.92 (s, 3 H), 3.00–2.97 (m, 3 H), 2.38–2.05 (m, 2 H), 2.34 (s, 3 H), 2.05 (m, 2 H), 1.56 (m, 2 H). ¹³C NMR (100 MHz, CDCl₃) δ 195.8, 173.7, 166.6, 157.4, 110.2, 104.7, 86.6, 56.8, 56.1, 56.0, 46.7, 31.7, 29.5; MS (ESI) m/z 292 [M + H⁺]. Anal. (C₁₆H₂₁NO₄·¹/₄H₂O) C, H, N.

4,6-Dihydroxy-7-(1-methyl-piperidin-4-yl)-2-[1-phenyl-meth-(E)-ylidene]-benzofuran-3-one (4). To a solution of **13** (200 mg, 0.7 mmol) and benzaldehyde (72 mg, 0.7 mmol) in ethanol (10 mL) was added potassium hydroxide (75 mg, 1.3 mmol) at room temperature. The reaction mixture was stirred for 1 h; the product, which precipitated, was filtered and directly mixed with pyridinium hydrochloride (1500 mg, 13 mmol) and heated at 180 °C for 3 h. The reaction mixture was allowed to cool to room temperature and was dissolved in methanol/water (1:1, 3 mL). Reverse phase MPLC chromatography afforded after lyophilization the trifluoroacetic salt of **4** as an orange powder (98 mg, 30%): HPLC t_R = 5.61 min; ¹H NMR (500 MHz, DMSO-*d*₆) δ 11.11 (s, 1 H), 10.89 br s, 1 H), 9.30 (br s, 1 H), 7.89 (d J = 7.6 Hz, 2 H), 7.51 (m, 2 H), 7.42 (m, 1 H), 6.61 (s, 1 H), 6.20 (s, 1 H), 3.53 (m, 2 H), 3.10 (m, 2 H), 2.83 (d, J = 4.5 Hz, 3 H), 2.39 (m, 2 H), 1.91 (m, 2 H); ¹³C NMR (125 MHz, DMSO-*d*₆) δ 179.3, 165.4, 165.0, 156.7, 147.4, 132.3, 130.7, 129.1, 129.0, 108.0, 104.7, 102.5, 98.0, 54.3, 43.0, 30.3, 27.5; LCMS (ESI) t_R = 6.12 min, m/z 352.2 [M + H⁺]. HRMS (ESI) calcd for C₂₁H₂₁NO₄ [M + H⁺] m/z 352.149; found, 352.1550.

2-[1-(2-Chloro-phenyl)-meth-(E)-ylidene]-4,6-dihydroxy-7-(1-methyl-piperidin-4-yl)-benzofuran-3-one (5). Following the procedure used in the preparation of compound **4**, **5** was prepared from **13** and 2-chlorobenzaldehyde: 30% yield; HPLC t_R = 6.13 min; ¹H NMR (500 MHz, DMSO-*d*₆, 373 K) δ

10.45 (br s 3H), 8.17 (d J = 7.5 Hz, 1 H), 7.56 (d J = 8.0 Hz, 1 H), 7.52 (m, 1 H), 7.42 (m, 1 H), 6.84 (s, 1 H), 6.23 (s, 1 H), 3.50 (m, 2 H), 3.21 (m, 1H), 3.0 (m obscured by water peak), 2.83 (s, 3 H), 2.41 (m, 2 H), 1.93 (m, 2 H); ¹³C NMR (125 MHz, DMSO-*d*₆) δ 179.0, 165.7, 165.0, 157.0, 148.6, 133.8, 131.4, 130.4, 129.9, 129.9, 128.1, 104.9, 102.2, 102.1, 98.1, 54.2, 43.0, 30.3, 24.4; LCMS (ESI) t_R = 9.13 min, m/z 386.2 [M + H⁺]. HRMS (ESI) calcd for C₂₁H₂₀ClNO₄ [M + H⁺] m/z 386.1159; found, 386.1159.

4,6-Dihydroxy-7-(1-methyl-piperidin-4-yl)-2-[1-(4-nitro-phenyl)-meth-(E)-ylidene]-benzofuran-3-one (6). Following the procedure used in the preparation of compound **4**, **6** was prepared from **13** and 4-nitrobenzaldehyde: 17% yield; HPLC t_R = 5.96 min; ¹H NMR (500 MHz, DMSO-*d*₆) δ 11.26 (s, 1 H), 11.06 (s, 1 H), 9.25 (br s, 1 H), 8.36 (d J = 8.9 Hz, 2 H), 8.13 (d J = 8.9 Hz, 2 H), 6.76 (s, 1 H), 6.22 (s, 1 H), 3.55 (m, 2 H), 3.17 (m, 1H), 3.10 (m, 2 H), 2.83 (d, J = 4.1 Hz, 3 H), 2.36 (m, 2 H), 1.91 (m, 2 H); ¹³C NMR (125 MHz, DMSO-*d*₆) δ 178.9, 165.8, 165.0, 157.1, 149.3, 146.6, 139.3, 131.3, 130.7, 124.2, 123.7, 105.2, 105.1, 102.1, 98.2, 54.3, 43.1, 30.2, 27.5; LCMS (ESI) t_R = 5.74 min, m/z 397.2 [M+H⁺]; HRMS (ESI) calcd for C₂₁H₂₀N₂O₆ [M+H⁺] m/z 397.1400; found, 397.1397.

4-[4,6-Dihydroxy-7-(1-methyl-piperidin-4-yl)-3-oxo-3H-benzofuran-(2E)-ylidenemethyl]-benzenesulfonamide (7). Following the procedure used in the preparation of compound **4**, **7** was prepared from **13** and 4-formyl-benzenesulfonamide: 14% yield; HPLC t_R = 4.83 min; ¹H NMR (500 MHz, DMSO-*d*₆) δ 11.19 (s, 1 H), 10.99 (s, 1 H), 9.27 (br s, 1 H), 8.05 (d J = 8.5 Hz, 2 H), 7.95 (d J = 8.5 Hz, 2 H), 7.44 (s, 2H), 6.66 (s, 1 H), 6.21 (s, 1 H), 3.54 (m, 2 H), 3.19 (m, 1 H), 3.12 (m, 2 H), 2.84 (d J = 4.5, 2 H), 2.38 (m, 2 H), 1.91 (m, 2 H); ¹³C NMR (125 MHz, DMSO-*d*₆) δ 179.1, 165.6, 165.0, 156.9, 148.5, 143.6, 135.6, 130.8, 126.4, 106.1, 104.9, 102.2, 98.1, 54.3, 43.0, 30.2, 27.4; LCMS (ESI) t_R = 5.39 min, m/z 431.2 [M + H⁺]. HRMS (ESI) calcd for C₂₁H₂₂N₂O₆S [M + H⁺] m/z 431.1277; found, 431.1278.

2-[1-(4-Bromo-phenyl)-meth-(E)-ylidene]-4,6-dimethoxy-7-(1-methyl-piperidin-4-yl)-benzofuran-3-one (14). To a solution of **13** (582 mg, 2 mmol) and 4-bromobenzaldehyde (370 mg, 2 mmol) in ethanol (10 mL) was added potassium hydroxide (224 mg, 4 mmol) at room temperature. The reaction mixture was stirred for 1 h; the product, which precipitated, was filtered to afford pure **14** as a yellow crystalline compound (375 mg, 41%): mp 220–223 °C; HPLC t_R = 6.99 min; ¹H NMR (400 MHz, DMSO-*d*₆) δ 7.9 (d J = 8.6 Hz, 2 H), 7.63 (d J = 8.6 Hz, 2 H), 6.68 (s, 1 H), 6.44 (s, 1 H), 3.97 (s, 3 H), 3.95 (s, 3 H), 3.05–2.89 (m, 3 H), 2.32–2.19 (m, 2 H), (2.26 s, 3H), 1.94 (m, 2 H), 1.55 (m, 2 H); ¹³C NMR (100 MHz, DMSO-*d*₆) δ 178.9, 165.8, 164.3, 157.6, 147.2, 122.3, 109.5, 107.1, 103.6, 91.5, 56.6, 56.1, 56.0, 46.1, 31.4, 29.3. HRMS (ESI) calcd for C₂₃H₂₄BrNO₄ [M + H⁺] m/z 458.0967; found, 458.0965.

4,6-Dimethoxy-2-[1-[4-(4-methyl-piperazin-1-yl)-phenyl]-meth-(E)-ylidene]-7-(1-methyl-piperidin-4-yl)-benzofuran-3-one (15). A solution of **14** (92 mg, 0.2 mmol), 1-methylpiperazine (42 mg, 0.42 mmol), Pd₂(dba)₃ (5 mg, 0.006 mmol), racemic-BINAP (9 mg, 0.0014 mmol), and cesium carbonate (150 mg, 0.46 mmol) was refluxed in dioxan (2 mL) under argon for 12 h. The reaction mixture was diluted with ethyl acetate washed with brine, dried over magnesium sulfate, concentrated under reduced pressure, and crystallized from 2-propanol to afford the dimethoxy intermediate as an orange crystalline compound (53 mg, 55%): HPLC t_R = 4.96 min; ¹H NMR (500 MHz, DMSO-*d*₆, 353 K) δ 7.78 (d J = 8.6 Hz, 2 H), 7.06 (d J = 8.6 Hz, 2 H), 6.59 (s, 1 H), 6.45 (s, 1 H), 3.98 (s, 3 H), 3.96 (s, 3 H), 3.39–3.18 (m, 6 H), 2.63–2.29 (m, 13 H), 1.79 (m, 2 H), 1.04 (m, 2 H). HRMS (ESI) calcd for C₂₈H₃₅N₃O₄ [M + H⁺] m/z 458.0967; found, 458.0965.

4,6-Dihydroxy-2-[1-[4-(4-methyl-piperazin-1-yl)-phenyl]-meth-(E)-ylidene]-7-(1-methyl-piperidin-4-yl)-benzofuran-3-one (8). Compound **15** (32 mg, 0.067 mmol) was mixed with pyridinium hydrochloride (50 mg, 0.43 mmol) and heated at 180 °C for 3 h. The reaction mixture was allowed to cool to room temperature and was dissolved in methanol–water (1:1, 1 mL). Reverse phase MPLC chromatography

afforded after lyophilization the bis-trifluoroacetic salt of **8** as a yellow powder (16 mg, 40%): HPLC $t_R = 4.44$ min; $^1\text{H NMR}$ (500 MHz, DMSO- d_6) δ 11.01 (s, 1 H), 10.77 (s, 1 H), 9.87 (br s, 1 H), 9.40 (br s, 1 H), 7.82 (d $J = 9.0$ Hz, 2 H), 7.12 (d $J = 9.0$ Hz, 2 H), 6.57 (s, 1 H), 6.19 (s, 1 H), 3.99 (br s, 2 H), 3.65–2.95 (m, 11 H), 2.88 (s, 3 H), 2.83 (m, 3 H), 2.40 (m, 2 H), 1.90 (m, 2 H); $^{13}\text{C NMR}$ (100 MHz, DMSO- d_6) δ 179.2, 164.8, 164.6, 156.4, 149.6, 145.9, 132.2, 123.3, 115.5, 108.6, 104.4, 102.8, 97.9, 54.3, 52.0, 44.6, 43.0, 42.1, 30.3, 27.4; LCMS (ESI) $t_R = 9.24$ min (5% B to 40% B over 9 min then 40% for 5 min), m/z 450.3 $[\text{M} + \text{H}^+]$. HRMS (ESI) calcd for $\text{C}_{26}\text{H}_{31}\text{N}_3\text{O}_4$ $[\text{M} + \text{H}^+]$ m/z 450.2393; found, 450.2395.

Molecular Modeling. The coordinates of CDK2 in complex with ATP (PDB code 1HCK) were used to construct the models shown in Figures 1 and 2 and to perform the binding energy calculations. Flavopiridol and the benzofuranone mimics were manually docked in the ATP binding site, and the resulting ligand–protein complexes were energy minimized using the AMBER* force field in conjunction with the GB/SA water solvation model as implemented in MacroModel.³³ Only residues of the ATP pocket within 12 Å of the initial position of the ligand were included in the calculations. During the minimization, the protein atoms were restrained to their crystallographic positions by a force constant of 24 kcal mol⁻¹ Å⁻¹ except for the side chain of Lys 89 which was allowed to move freely. A sufficient number of iterations of Polak-Ribiere conjugate gradient minimization was applied to reach a value of the energy gradient less than 0.002 kcal mol⁻¹ Å⁻¹. For the complex with compound **8**, the initial position of the side chain of Lys 89 was manually modified in order to remove a close contact with the piperazyl substituent.

The binding energy of each modeled compound was calculated according to the following formula (AMBER*/H₂O/GBSA energies)

$$E_{\text{binding}} = E_{\text{complex}} - E_{\text{ligand}} - E_{\text{enzyme}} \quad (1)$$

where E_{ligand} is the energy of the ligand minimized to the nearest local minimum after extraction of the minimized complex and E_{enzyme} is the energy of the enzyme in the minimized complex. Binding energies calculated with this formula do not take into account entropy factors, the deformation energy (conformational) of the ligand induced by complexation calculated with the global minimum in solution as reference, and the deformation energy of the enzyme. For the comparison of the structurally very close and conformationally rigid analogues under investigation here, it is reasonable to assume that these terms are constant and therefore do not need to be calculated.

References

- Mani, S.; Wang, C.; Wu, K.; Francis, R.; Pestell, R. Cyclin-dependent kinase inhibitors: novel anticancer agents. *Expert Opin. Invest. Drugs* **2000**, *9*, 1849–1870.
- Fischer, P. M.; Lane, D. P. Inhibitors of cyclin-dependent kinases as anti-cancer therapeutics. *Curr. Med. Chem.* **2000**, *7*, 1213–1245.
- Rosania, G. R.; Chang, Y. T. Targeting hyperproliferative disorders with cyclin dependent kinase inhibitors. *Expert Opin. Ther. Pat.* **2000**, *10*, 215–230.
- Sielecki, T. M.; Boylan, J. F.; Benfield, P. A.; Trainor, G. L. Cyclin-dependent kinase inhibitors: useful targets in cell cycle regulation. *J. Med. Chem.* **2000**, *43*, 1–18.
- Gray, N.; Detivaud, L.; Doerig, C.; Meijer, L. ATP-site directed inhibitors of cyclin-dependent kinases. *Curr. Med. Chem.* **1999**, *6*, 859–875.
- Kelland, L. R. Flavopiridol, the first cyclin-dependent kinase inhibitor to enter the clinic: current status. *Expert Opin. Invest. Drugs* **2000**, *9*, 2903–2911.
- Senderowicz, A. M.; Sausville, E. A. Preclinical and clinical development of cyclin-dependent kinase modulators. *J. Natl. Cancer Inst.* **2000**, *92*, 376–387.
- Senderowicz, A. M.; Headlee, D.; Stinson, S. F.; Lush, R. M.; Kalil, N.; Villalba, L.; Hill, K.; Steinberg, S. M.; Figg, W. D.; Tompkins, A.; Arbuck, S. G.; Sausville, E. A. Phase I trial of continuous-infusion flavopiridol, a novel cyclin-dependent kinase inhibitor, in patients with refractory neoplasms. *J. Clin. Oncol.* **1998**, *16*, 2986–2999.
- Murthi, K. K.; Dubay, M.; McClure, C.; Brizuela, L.; Boisclair, M. D.; Worland, P. J.; Mansuri, M. M.; Pal, K. Structure–activity relationship studies of flavopiridol analogues. *Bioorg. Med. Chem. Lett.* **2000**, *10*, 1037–1041.
- Kim, K. S.; Sack, J. S.; Tokarski, J. S.; Qian, L.; Chao, S. T.; Leith, L.; Kelly, Y. F.; Misra, R. N.; Hunt, J. T.; Kimball, S. D.; Humphreys, W. G.; Wautlet, B. S.; Mulheron, J. G.; Webster, K. R. Thio- and Oxoflavopiridols, Cyclin-Dependent Kinase 1-Selective Inhibitors: Synthesis and Biological Effects. *J. Med. Chem.* **2000**, *43*, 4126–4134.
- Webster, K. R. Therapeutic Potential of Targeting the Cell Cycle. *Chem. Res. Toxicol.* **2000**, *13*, 940–943.
- De Azevedo, W. F.; Mueller-Dieckmann, H. J.; Schulze-Gahmen, U.; Worland, P. J.; Sausville, E.; Kim, S. H. Structural basis for specificity and potency of a flavonoid inhibitor of human CDK2, a cell cycle kinase. *Proc. Natl. Acad. Sci. U.S.A.* **1996**, *93*, 2735–2740.
- In CDK2, Glu 81 and Leu 83 are the two residues that constantly provide bi- or tri-dentate hydrogen bonds with the inhibitor, whatever its structure (see ref 5).
- Schulze-Gahmen, U.; Brandsen, J.; Jones, H. D.; Morgan, D. O.; Meijer, L. Multiple modes of ligand recognition: crystal structures of cyclin-dependent protein kinase 2 in complex with ATP and two inhibitors, olomoucine and isopentenyladenine. *Proteins: Struct., Funct., Genet.* **1995**, *22*, 378–391.
- Inhibitor hydrogen bonds to Lys 89 and Asp 86 have previously been observed in particular in the structure of CDK2 in complex with the inhibitor purvalanol B: Gray, N. S.; Wodicka, L.; Thunnissen, A. M.; Norman, T. C.; Kwon, S.; Espinoza, F. H.; Morgan, D. O.; Barnes, G.; LeClerc, S.; Meijer, L.; Kim, S. H.; Lockhart, D. J.; Schultz, P. G. Exploiting chemical libraries, structure, and genomics in the search for kinase inhibitors. *Science* **1998**, *281*, 533–538.
- Sarbagya, D. P.; Rangachari, K.; Mazumdar, A. K. D.; Banerji, K. D. Synthesis of Pyrido[3,2-*b*]benzofurans. *Indian J. Chem. B* **1986**, *25*, 891–893.
- Brady, B. A.; Kennedy, J. A.; O'Sullivan, W. I. The Configuration of Aurones. *Tetrahedron* **1973**, *29*, 359–362.
- Hastings, J. S.; Heller, H. G. Stereochemistry of aurones [2-(substituted benzylidene)-3(2H)-benzofuranones]. *J. Chem. Soc., Perkin Trans. 1* **1972**, 2128–2132.
- Mansuri, M. M.; Murthi, K. K.; Pal, K. Preparation of analogs of chromones as inhibitors of cyclin-dependent kinases. WO 9716447, 1997; *Chem. Abstr.* **1997**, *127*, 50539.
- Van Es, T.; Statskun, B. Aldehydes from Aromatic Nitriles: *p*-Formylbenzenesulfonamide. *Org. Synth.* **1971**, *51*, 20–23.
- Wolfe, J. P.; Buchwald, S. L. Improved functional group compatibility in the palladium-catalyzed amination of aryl bromides. *Tetrahedron Lett.* **1997**, *38*, 6359–6362.
- Imbach, P.; Capraro, H. G.; Furet, P.; Mett, H.; Meyer, T.; Zimmermann, J. 2,6,9-Trisubstituted purines: optimization towards highly potent and selective CDK1 inhibitors. *Bioorg. Med. Chem. Lett.* **1999**, *9*, 91–96.
- Leclerc, S.; Garnier, M.; Hoessel, R.; Marko, D.; Bibb, J. A.; Snyder, G. L.; Greengard, P.; Biernat, J.; Wu, Y. Z.; Mandelkow, E. M.; Eisenbrand, G.; Meijer, L. Indirubins inhibit glycogen synthase kinase-3 beta and CDK5/p25, two protein kinases involved in abnormal tau phosphorylation in Alzheimer's disease. A property common to most cyclin-dependent kinase inhibitors? *J. Biol. Chem.* **2001**, *276*, 251–260.
- Zimmermann, J.; Caravatti, G.; Mett, H.; Meyer, T.; Muller, M.; Lydon, N. B.; Fabbro, D. Phenylamino-pyrimidine (PAP) derivatives: a new class of potent and selective inhibitors of protein kinase C (PKC). *Arch. Pharm. (Weinheim)* **1996**, *329*, 371–376.
- Bold, G.; Altmann, K. H.; Frei, J.; Lang, M.; Manley, P. W.; Traxler, P.; Wietfeld, B.; Brueggen, J.; Buchdunger, E.; Cozens, R.; Ferrari, S.; Furet, P.; Hofmann, F.; Martiny-Baron, G.; Mestan, J.; Roesel, J.; Sills, M.; Stover, D.; Acemoglu, F.; Boss, E.; Emmenegger, R.; Laesser, L.; Masso, E.; Roth, R.; Schlachter, C.; Vetterli, W.; Wyss, D.; Wood, J. M. New Anilinothalazines as Potent and Orally Well Absorbed Inhibitors of the VEGF Receptor Tyrosine Kinases Useful as Antagonists of Tumor-Driven Angiogenesis. *J. Med. Chem.* **2000**, *43*, 2310–2323.
- Trinks, U.; Buchdunger, E.; Furet, P.; Kump, W.; Mett, H.; Meyer, T.; Mueller, M.; Regenass, U.; Rihs, G. Dianilinothalazines: Potent and Selective, ATP–Competitive Inhibitors of the EGF-Receptor Protein Tyrosine Kinase. *J. Med. Chem.* **1994**, *37*, 1015–1027.
- Flavopiridol is 10-fold more potent in inhibiting CDK2 than its *des*-chloro analogue. Losiewicz, M. D.; Carlson, B. A.; Sausville, E. A.; Naik, R. G.; Narayanan, V. L.; Worland, P. J. Inhibition of CDK2 by flavopiridol and structural analogs. *Proc. Am. Assoc. Cancer Res. (86th Meet.)*, **1995**, *36*, 35.

- (28) Soni, R.; O'Reilly, T.; Furet, P.; Muller, L.; Stephan, C.; Zumstein-Mecker, S.; Fretz, H.; Fabbro, D.; Chaudhuri, B. Selective in vivo and in vitro effects of a small molecule inhibitor of cyclin-dependent kinase 4. *J. Natl. Cancer Inst.* **2001**, *93*, 436–446.
- (29) Soni, R.; Fretz, H.; Muller, L.; Schoepfer, J.; Chaudhuri, B. Novel Cdk Inhibitors Restore TGF- β Sensitivity in Cdk4 Overexpressing Epithelial Cells. *Biochem. Biophys. Res. Commun.* **2000**, *272*, 794–800.
- (30) Soni, R.; Muller, L.; Furet, P.; Schoepfer, J.; Stephan, C.; Zumstein-Mecker, S.; Fretz, H.; Chaudhuri, B. Inhibition of Cyclin-Dependent Kinase 4 (Cdk4) by Fascaplysin, a Marine Natural Product. *Biochem. Biophys. Res. Commun.* **2000**, *275*, 877–884.
- (31) Rialet, V.; Meijer, L. A New Screening Test for Antimitotic Compounds Affinity-Immobilized on p13^{suc1}-Coated Microtitration Plates. *Anticancer Res.* **1991**, *11*, 1581–1590.
- (32) Shih, H.; Deng, L.; Carrera, C. J.; Adachi, S.; Cottam, H. B.; Carson, D. A. Rational design, synthesis and structure–activity relationships of antitumor (E)-2-benzylidene-1-tetralones and (E)-2-benzylidene-1-indanones. *Bioorg. Med. Chem. Lett.* **2000**, *10*, 487–490.
- (33) Mohamadi, F.; Richards, N. G. J.; Guida, W. C.; Liskamp, R.; Lipton, M.; Caufield, C.; Chang, G.; Hendrickson, T.; Still, W. C. MacroModel – an integrated software system for modeling organic and bioorganic molecules using molecular mechanics. *J. Comput. Chem.* **1990**, *11*, 440–467.

JM0108348